ELSEVIER

Brain Research 866 (2000) 313–325

BRAIN RESEARCH INTERACTIVE

www.elsevier.com/locate/bres

Interactive report

Intracerebral hemodynamics probed by near infrared spectroscopy in the transition between wakefulness and sleep[1]

Arthur J. Spielman[a,*], Gang Zhang[b], Chien-Ming Yang[a], Paul D'Ambrosio[a], Shiro Serizawa[a], Massanori Nagata[a], Hans von Gizycki[a], Robert R. Alfano[b]

[a]*Sleep Disorders Center, Department of Psychology, The City College of the City University of New York, 138th Street and Convent Avenue, New York, NY 10031, USA*

[b]*Institute for Ultrafast Spectroscopy and Lasers, New York State Center for Advanced Technology for Ultrafast Photonic Materials, Applications Department of Electrical Engineering and Physics, The City College of the City University of New York, 138th Street and Convent Avenue, New York, NY 10031, USA*

Accepted 29 March 2000

Abstract

Previous imaging studies have shown that cerebral metabolism is gradually reduced at the beginning of sleep. Few studies have examined the sleep state transition periods from wakefulness to sleep and sleep to wakefulness. The current study used the Near Infrared Spectroscopy (NIRS) technique to describe the intracerebral hemodynamics at the frontal pole in the circumscribed period between wakefulness and sleep. Nine healthy young adults were studied during afternoon naps. Optical probes were placed on the forehead and EEG electrodes on the scalp. At sleep onset oxygenated hemoglobin (oxy-Hb) was reduced ($P<0.01$) and deoxygenated hemoglobin (deoxy-Hb) showed a near significant reduction ($P<0.063$). At sleep offset there were increases in oxy-Hb ($P<0.005$) and deoxy-Hb ($P<0.05$). In 18 of 26 transitions to sleep there was a coordinated fall in both NIRS parameters, we call the Switch Point, that lasted a mean of 3.6 s. In 32 of 36 transitions to wakefulness there was an analogous Switch Point that lasted a mean of 3.4 s. Before and after the Switch Point, changes were small and the relationship between oxy-Hb and deoxy-Hb was a combination of parallel and reciprocal fluctuations. A synchronized, parallel and short-lived change in oxy-Hb and deoxy-Hb is a discrete event in the transition period between wakefulness and sleep. The concentration of these light absorbing molecules is abruptly set to a new level at sleep–wake transitions and probably reflects the different perfusion demands of these states. © 2000 Elsevier Science B.V. All rights reserved.

Themes: Other systems of the CNS

Topics: Brain metabolism and blood flow

Keywords: Near infrared spectroscopy; Sleep; Cerebral metabolism

1. Introduction

New techniques for functional imaging of the brain have great promise for elucidating basic neurobiological mechanisms (see [66]). While the process of waking activation (see [54]) and sleep-related changes [1,3,4,10,22,24,33,36–38,45,46,57,67] have received much attention, relatively unexplored by neuroimaging techniques is the boundary between wakefulness and sleep. Quantitative EEG brain mapping has shown that around the time of sleep onset, alpha frequency disappears and theta frequency increases especially along the midline and in posterior regions [75]. Increased delta and decreased beta activity as well as increased EEG power have also been observed [4,44,52]. Given these distinct EEG changes and the profound and global changes in consciousness and functional capacity in the transition to sleep, it is somewhat surprising that the reduction in cerebral metabolic rate and cerebral blood flow are small and gradual [16,32,46,57]. The characterization of the sleep onset process as incremental may be a function of the limitations of the techniques employed (see [51,55]). To better understand the sleep state transition process the present study employed near infrared spec-

[1]Published on the World Wide Web on 25 April 2000.

*Corresponding author. Tel.: +1-212-832-1544; fax: +1-212-650-5722.

E-mail address: thrilla834@aol.com (A.J. Spielman)

0006-8993/00/$ – see front matter © 2000 Elsevier Science B.V. All rights reserved.
PII: S0006-8993(00)02320-9

troscopy (NIRS) to characterize regional cerebral hemodynamics during the transitions between wakefulness and sleep and sleep and wakefulness.

Near infrared light passes through extracranial tissue into the brain and a portion of the light delivered scatters back to a sensor with valuable information concerning intracerebral attenuation of light [27]. The light attenuation can be attributed mainly to the fluctuating levels of several key light absorbing molecules: oxygenated hemoglobin (oxy-Hb), deoxygenated hemoglobin (deoxy-Hb), and cytochrome oxidase ([5,9], see [6]). The NIRS technique yields changes in levels of these chromophores by illuminating a small volume of the intracerebral tissue and vasculature. The use of NIRS in combination with fMRI, trascranial doppler, direct blood assays and other techniques has yielded convergent validity of the optical method [8,12,23,29,30,39,40,42,43,53,60,62,65,76]. Advantages of NIRS of the brain over other imaging techniques include, measurement of specific biochemical markers, localization to a fairly superficial layer of gray matter and a rapid response of approximately 1 s or less. The technique is non-invasive, may be used for extended periods of time and the equipment is small, portable and, unlike fMRI, may be used in conjunction with other techniques such as EEG. A number of non-invasive NIRS methods are available and they are the only means to directly measure changes in the concentration and oxygenation of hemoglobin in the brain from the intact skull ([2,5,9], see [6]). The reflectance mode NIRS apparatus used in this study can fit on a small cart, may be used at the bedside of patients and provides continuous online information for hours. In clinical applications the monitoring of hemodynamics may be critical in the brain, which is vulnerable to prolonged hypoxia. While the high standard necessary to impact clinical decision making has not yet been achieved by NIRS, advances in technology are likely to enhance the already valuable information that can be obtained [19,61,63,76]. Relatively inexpensive compared to other imaging techniques, the cost of the apparatus excluding the computer was less than $10,000.

Past studies of NIRS during the transition to sleep have described a number of patterns. As subjects fell asleep an oxy-Hb decrease and deoxy-Hb increase from a frontal location were accompanied by either a decrease or no change in total hemoglobin (t-Hb) [25]. Similar findings were obtained with NIRS placed at frontal and central derivations but inverse changes, oxy-Hb increase and deoxy-Hb decrease, were recorded from the occipital region [59]. These past studies did not specify the time period examined, conducted no statistical analysis of the data and did not evaluate the complimentary transitional state from sleep to wakefulness. The present study was designed to address all of these limitations and describe the pattern of NIRS changes in the boundary between sleep and wakefulness.

2. Materials and methods

2.1. Subjects

Nine healthy individuals with an average age of 30.3 years (range 22–52), 7 male, 2 female, served as subjects. Subjects restricted their sleep to about 4 h on the night before the day of the experiment in order to facilitate sleep during the day. The study was approved by the City College of New York's Institutional Review Board and written documentation of informed consent was obtained from subjects.

2.2. Instrumentation

Fig. 1 shows a schematic of the approach. The optical fiber probes were placed 3 cm apart, embedded in an elastic headband with a perpendicular orientation to the surface of the forehead. Symmetrically positioned across the midline, the input probe was to the left (near Fp2) and the detector probe to the right (near Fp1). Both probes were approximately equidistant from the eyebrows and hairline. We chose to apply optodes to the forehead rather than the scalp because the hair in the scalp attenuates light significantly and reduces the signal to noise ratio. In

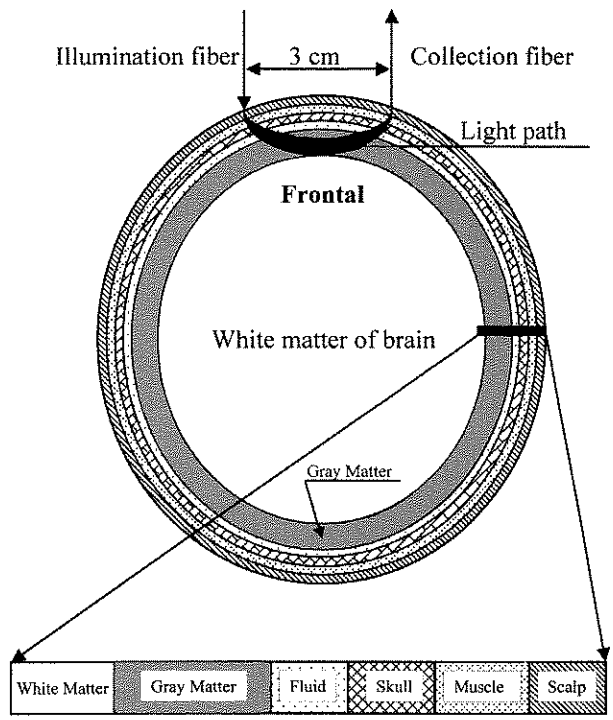

Fig. 1. Schematic of the near infrared probes and light path. A schematic representation of the NIRS set-up used to monitor local intracerebral brain activity is depicted. The view is looking down on the top of the head. The theoretical light path through the head represents only the major portion of the light delivered that scatters back and is detected in the collection fiber.

addition, there is evidence that the frontal lobes and midline structures show early changes in the transition to sleep [20,75] and we were interested in the boundary state between wakefulness and sleep.

Two diode lasers delivered near infrared light at 830 nm and 780 nm. These wavelengths were selected because they lie on each side of the isosbestic point of the oxy-Hb and deoxy-Hb absorption spectra at ~800 nm. The light was propagated through a 1.125 mm optical fiber to the subject at about 0.25 mw (0.1 mw for 780 nm and 0.15 mw for 830 nm) at the output point. The output power of the fiber was set below 0.32 mw/cm^2 for each wavelength. For these parameters of low power laser light no safety precautions are required for less than 8 h of use [31].

A 5 mm diameter liquid optical waveguide was used to collect the optical signal. The collected optical signal was passed through a wide band filter with center wavelength of 800 nm to remove the environmental light noise and transformed to an electrical signal by a single photo multiplier tube (PMT) model R943. Two PC-board lock-in amplifiers (Ithaca model 3981) were used for detection. The beam was chopped at 367 Hz for oxy-Hb and 600 Hz for deoxy-Hb. The two wavelength optical signals were detected at these chopped frequencies and read out from the two lock-in outputs.

Bipolar EEG signals and the NIRS signals were simultaneously recorded by connecting to a polygraph recorder and a PC computer based digital recorder. Analog data from the EEG amplifier's J6 output was digitized at 12 bit at 256 Hz by a Microstar Laboratories DAP 1200 signal processing card with dynamic range of ±5 V. A Pentium 166 MHz PC was used for data collection by data acquisition software (Dapf©, von Gizycki, 1996). A Grass 7D polygraph with 7P511 amplifiers was used to acquire electrophysiological data. Amplifier settings were as follows: Sensitivity=5 UV/mm, high filter=1 K, low filter=0.30. The following seven-channel montage was used according to the international 10–20 system [26]: C_3–A_1A_2, C_4–A_2, O_1–F_Z, O_2–F_Z, Left outer canthus — A_1, Right outer canthus — A_2, and bipolar mentalis muscle for chin electromyogram.

Wavelengths above and below 805 nm provide measures of both oxy-Hb and deoxy-Hb concentrations [27]. Employing the absorption coefficients (Table 1, [68]) at optical wavelengths of 780 and 830 nm the change in the concentration of oxy-Hb and deoxy-Hb results from an analysis of the amount of light scattered back from the brain using the following linear equations (OD stands for optical density):

$$\Delta\text{deoxy-Hb} = 7.9\text{OD}_{780} - 5.8\Delta\ \text{OD}_{830} \quad (1)$$

$$\Delta\text{oxy-Hb} = 9.1\text{OD}_{830} - 6.8\Delta\ \text{OD}_{780} \quad (2)$$

$$\Delta t\text{-Hb} = \Delta\text{deoxy-Hb} + \Delta\text{oxy-Hb} = 1.1\text{OD}_{780} + 3.3\Delta\ \text{OD}_{830} \quad (3)$$

The path of the light that is scattered back and collected has been assumed to be banana shaped, penetrating approximately 1.5–3.0 cm with an optode separation of 3 cm (Fig. 1; [23,29,41,49,71,74]). Lacking knowledge of a number of parameters, including the path length and differential absorption by different layers of tissue, it is not possible to determine the absolute concentration of the chromophores ([5,9], see [6]). The NIRS values are therefore in arbitrary units, calculated as follows: Within each segment analyzed the initial NIRS values are set to zero and all changes are relative to the data set within the segment.

The total hemoglobin (t-Hb) value is the arithmetic sum of oxy-Hb and deoxy-Hb. Although the value of t-Hb is not independent of either oxy-Hb or deoxy-Hb we will statistically analyze this parameter separately because of its correspondence to cerebral blood volume (see [72]). Details of the NIRS analysis, equipment, demonstration of the current approach in the periphery and correspondence between the current and an established technique [64] in an animal preparation will be presented elsewhere.

Table 1
Hemoglobin absorption coefficients at two wavelengths, 780 nm and 830 nm[a]

Wavelength (nm)	deoxy-Hb	oxy-Hb	ΔOD (deoxy-Hb minus oxy-Hb)
780	0.28	0.18	+0.1
830	0.21	0.245	−0.035

[a] Abbreviations are as follows: oxygenated hemoglobin (oxy-Hb), deoxygenated hemoglobin (deoxy-Hb), change (Δ) in optical density (OD). OD~mM/cm [68].

2.3. Procedure

The napping protocol began between noon and 2 pm. Following preliminary calibrations and 3 min of waking recording with eyes alternatively opened and closed the room lights were turned off, the door of the sound attenuated room closed and the subject was told to go to sleep. When the polygraphic record indicated that the subject was in stage 2 sleep for over 30 s, the investigator woke the subject by calling his or her name on the intercom. The subject was kept awake for at least 30 s and then told to return to sleep. Subjects were encouraged to fall asleep more than once so that multiple sleep onsets and sleep offsets could be collected.

2.4. Data analytic strategy

The data analytic strategy was analogous for the wakefulness to sleep and the sleep to wakefulness transition. To

avoid repetition we will describe the complete procedure for only the wakefulness to sleep period.

The analysis proceeded in steps (Table 2). The first step was visual identification of regions of the EEG data stream that were fairly clear and unidirectional in the transition from waking to sleep. An expert scorer (AJS) examined the polygraphic record and selected segments of 20–120 s in duration in which the transitions between waking and sleep were relatively unambiguous and there was no gross artifact present in the NIRS signal. Polygraphic segments in which alpha activity in the EEG waxed and waned were excluded from analysis. Within that region the point of human Scored Sleep Onset (Table 2, step 1) was defined based on polysomnographic criteria that mainly relied on the complete disappearance of alpha frequency on the EEG. In some cases, in which alpha was not abundant, this decision was based on the change to an EEG in the theta frequency range or mixed frequencies with amplitude greater than during unambiguous waking. Only a small number of wakefulness to sleep trials were included in the analysis. Our aim was to select portions of the record that demonstrated a continuous and uniform state change. Operationally, we selected segments that began with a relatively unbroken string of alpha in the EEG or an unambiguous waking EEG. In order to be selected for analysis this portion of wakefulness needed to be followed by continuous sleep for at least 20 s. In this sleep portion either alpha disappeared completely or there was a slowing to the theta range and a slight increase in EEG amplitude. These strict criteria for selection resulted in 26 sleep onsets selected for analysis in nine subjects.

The complementary transition, from sleep to wakefulness, was provoked by experimenters calling the subject's name over the intercom. Following the awakenings the typical pattern was a burst of high amplitude alpha in the EEG followed by a reduction in amplitude as wakefulness continued. The first appearance of alpha was defined as the point of human Scored Sleep Offset (Table 2, step 1). The

Table 2
Data analytic procedure and strategy for the examination of sleep onset and sleep offset[a]

Sequence	Method	Aim
Step 1	Expert sleep scorer determines the time when EEG alpha disappears (appears)	Point of human Scored Sleep Onset (Offset)
Step 2	Computer FFT identification of the point at which spectral power of EEG alpha is maximally reduced (increased)	Point of computer FFT Sleep Onset (Offset)
Step 3	Test if there is a difference between the points of Scored and FFT Sleep Onset (Offset)	Convergent validity
Step 4	Determine the maximal change in the concentration of oxy-Hb in the region of Scored Sleep Onset (Sleep Offset)	Confirm that the oxy-Hb response is a decrease at sleep onset (increase at sleep offset)
Step 5	Identify the point of maximal decrease (increase) in the concentration of oxy-Hb in the region of Scored Sleep Onset (Sleep Offset)	Locate the region of the NIRS signal to be used to identify the coordinated changes in the hemoglobin parameters
Step 6	Compare the magnitude and direction of the changes in the concentration of oxy-Hb, deoxy-Hb and t-Hb at the point of maximal decrease (increase) of oxy-Hb	Assess frontal cerebral hemodynamics associated with falling asleep (waking up)
Step 7	Determine the duration of the synchronized and parallel decrease (increase) in oxy-Hb and deoxy-Hb during the sleep onset (offset) period	Measure the duration of the hemodynamic Switch Point
Step 8	Assess the time delay between the Scored Sleep Onset (Offset) and the synchronized and parallel changes in the chromophores at the Switch Point.	Describe the timing of changes in NIRS in relation to state change
Step 9	Calculate the correlation between oxy-Hb and deoxy-Hb before, after, and at the Switch Point, in the sleep onset (offset) period	Describe the relationship between oxy-Hb and deoxy-Hb before, after and at the Switch Point

[a] The sequence of analyses used for examining sleep onset and, in the parentheses, the analogous strategy for sleep offset. The Fast Fourier Transform (FFT) of alpha power, maximal change in oxy-Hb, maximal decrease (and increase) in oxy-Hb, and changes in deoxy-Hb and total hemoglobin (t-Hb) were determined by a computer analysis of the difference in the average values between two successive 5 s windows.

point demarcating the change from sleep to wakefulness was clear and abrupt. In contrast to the small number of trials in which the wakefulness to sleep transition qualified, we were able to include a more representative sample of awakenings. We analyzed 37 transitions from sleep to wakefulness in nine subjects. The scorer was blind to the NIRS data when determining the points of Scored Sleep Onset and Offset. Each subject had at least one sleep onset and offset period that qualified for analysis.

The next step was to submit the regions of EEG data around the point of Scored Sleep Onset to a Fast Fourier Transform (FFT) analysis with a moving set of two 5-s windows (see the Computer analysis section below for algorithm). The change in alpha power was examined for the region starting 5 s before and ending 20 s after the point of Scored Sleep Onset. Computer derived FFT Sleep Onset was defined by the program as the point of maximal decrease in relative alpha power from the first to the second 5-s window (Table 2, step 2). The corresponding point of increased alpha power was called computer FFT Sleep Offset (Table 2, step 2). The third step was to compare the Scored Sleep Onset and computer FFT Sleep Onset and see how far apart they were in the time domain (Table 2, step 3). This comparison served as convergent validity of the two methods.

Standard sleep stage scoring requires analysis by an epoch of either 20 or 30 s [56]. In order to improve the temporal resolution in the evaluation of the timing of the hemoglobin changes we used two points; the point at which visual inspection detected the disappearance of alpha and the FFT analysis of maximum decrease in relative alpha power. While these criteria differ from standard sleep stage scoring, these EEG analyses resulted in the Switch Point from waking to sleep taking place out of conventionally scored Stage 1 sleep.

The decision to use two 5-s data windows to evaluate the EEG during the transition period between sleep and waking was based on the well known association between EEG alpha activity and wakefulness [56]. No such well-established temporal association has been demonstrated between NIRS parameters and sleep or wakefulness. Therefore, we systematically explored window sizes between 2 and 10 s. We found that all window sizes yielded consistent and significant findings for oxy-Hb changes at sleep onset and offset and deoxy-Hb changes at sleep offset. For deoxy-Hb at sleep onset, data window values below 5 s were unstable and values between 5 and 8 s were stable hovering near $P<0.06$ ranging between $P<0.05$ and $P<0.08$. We chose to use the 5-s data window because this was the shortest interval at which deoxy-Hb changes were stable.

It is well established that activation is associated with an increase in oxy-Hb (see [47,72]). A preliminary examination was conducted to confirm that oxy-Hb increases at sleep offset and decreases at sleep onset. This was accomplished by the program identifying the point where there was a maximal change (either increase or decrease) in the level of oxy-Hb from the first to the second 5-s window and statistically testing the change (Table 2, step 4). Once the expected increase in oxy-Hb at sleep offset was confirmed we re-examined the few trials in which the largest oxy-Hb change was not an increase at sleep offset. In these trials we visually selected that portion of the record that contained the largest oxy-Hb increase in the region of sleep offset (Table 2, step 5). Our aim was to examine the pattern of all NIRS changes that occur at the time of activation as indexed by the oxy-Hb rise as the subject woke up. The analogous procedure was conducted at sleep onset for the few trials in which the largest change in oxy-Hb was an increase. We then compared the magnitude and direction of the changes in oxy-Hb, deoxy-Hb and t-Hb that occurred at the same time (Table 2, step 6). For example, the point of maximal decrease in oxy-Hb in the region of falling asleep was used as the point around which deoxy-Hb and t-Hb values were calculated.

We visually selected that portion of the data stream at the decline in oxy-Hb at sleep onset in which there was also a decline in deoxy-Hb. We called this data segment in which both chromophores decreased simultaneously the Switch Point (Table 2, Step 7). The end of this synchronized decline was defined as the first bin (1 s) in which either of the chromophores was not lower than in the previous bin. This Switch Point was analyzed for the duration of the synchronized and parallel decreases in oxy-Hb and deoxy-Hb. The duration of the corresponding synchronized increases in the chromophores at sleep offset was also determined. We excluded from analysis the 8 sleep onset trials in which there was no simultaneous decrease in the two chromophores. In these trials only reciprocal changes in oxy-Hb and deoxy-Hb were present. Similarly, we excluded 5 sleep offset trials in which there was no synchronized increase in the chromophores. In addition, we calculated the time delay from Scored Sleep Onset (and Offset) to the synchronized hemoglobin changes (Table 2, step 8).

To describe the relative changes in oxy-Hb and deoxy-Hb in the region around sleep onset we calculated three correlation coefficients between oxy-Hb and deoxy-Hb, as follows (Table 2, step 9). In each of the three analyses we first standardized the data in the traditional manner [7] before performing the correlation. For a 4-s series of data at the Switch Point, for example, we took the mean of the four oxy-Hb 1-s bins and subtracted the mean from each of the bin values. We did the same for the four deoxy-Hb bins and then calculated the correlation between the transformed oxy-Hb and deoxy-Hb values. This preliminary transformation allowed us to perform an overall correlation across all trials. Three correlations were performed on different segments of the time series (Table 2, step 9). (1) A correlation was calculated between the two chromophores at the Switch Point, for the duration of the parallel and synchronized change in each sleep onset trial. (2) We

then selected the data for the 5 s prior to the onset of the Switch Point and calculated the correlation. (3) Similarly, we selected the segment for the 5 s immediately following the Switch Point, and calculated the correlation. The three corresponding correlations at sleep offset were also calculated.

Previous studies have shown that CBF levels during wakefulness are different before and after a long bout of sleep [10,16]. Our study examined changes before and after a short nap and did not directly compare wakefulness before and after the sleep period. The analyses were limited to the changes from wakefulness to sleep and sleep to wakefulness.

2.5. Computer analysis

A discrete FFT function was used to assess EEG power. The data was first detrended and then the power spectral density was computed using a 256 point FFT with 128 point hanning window. Frequency decomposition was performed using the MATLAB FFT function, and for EEG analysis, the squared absolute value of the output of this function was used as EEG power. In addition, EEG bands were computed as follows: beta (13 Hz $=<\beta<$ 30 hz), alpha (8 Hz $=<\alpha<$ 13 Hz), theta (4 Hz $=<\tau<$ 8 Hz), delta (0 Hz $=<\Delta<$ 4 Hz) and overall power was also computed.

As summarized in Eq. (1) below, alpha power of the EEG by FFT algorithm was analyzed to obtain the computer FFT Sleep Onset and Offset points. The EEG data stream was truncated to 1-s event data points. The sleep onset and offset points were determined by sampling segments of the data with a moving window as follows: Data was collected and averaged within each of two contiguous windows of 5 s. The entire data region of interest was sampled successively by moving the windows in 1-s increments and re-calculating the means of the two windows. When the difference between the averages of the first and second windows was the greatest the transition value separating the windows was defined as the point of computer FFT Sleep Onset or Sleep Offset.

$$V = \max(\text{mean data [second 5 s]} - \text{mean data [first 5 s]}) \quad (1)$$

Expressed by formula (1) V is the transition value (point of computer FFT Sleep Onset and Offset), mean data [second 5 s] and mean data [first 5 s] are the mean values of the data after and before the transition points respectively, within 5-s windows.

In the same manner, the maximal oxy-Hb response, maximal decrease in oxy-Hb at sleep onset, maximal increase in oxy-Hb at sleep offset and the corresponding changes in deoxy-Hb and t-Hb were obtained. The NIRS signals were averaged to 1-s event data points to eliminate high frequency noise.

3. Results.

Fig. 2 displays the long-term changes in the EEG and NIRS recordings for one subject. The top curve shows the EEG alpha power from electrode locations O_1–F_Z wakefulness labeled W and sleep labeled S. The lower curves present the hemoglobin concentration changes calculated from the NIRS signal at the forehead. The vertical lines mark the points of sleep state transitions at Scored Sleep Onset and Offset. As the subject fell asleep there were reductions in EEG alpha, oxy-Hb and t-Hb. The deoxy-Hb level appears little changed. In contrast, as the subject woke-up there were increases in EEG alpha, oxy-Hb and t-Hb. Again, the deoxy-Hb level appears little changed

3.1. Spontaneous transition from wakefulness to sleep

Fig. 3 displays the short-term changes in EEG alpha and hemoglobin concentration for one subject. In addition to the parameters presented in Fig. 2, this graph includes the cross correlation between oxy-Hb and deoxy-Hb for a 5 s

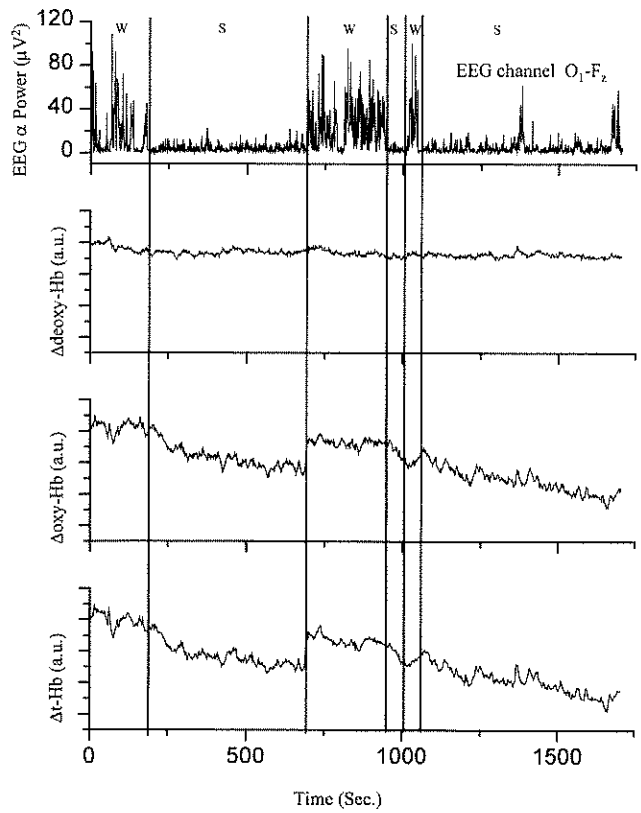

Fig. 2. Long term changes in EEG and NIRS between sleep and waking. Illustration of the relative changes in hemoglobin concentration (oxygenated hemoglobin [oxy-Hb], deoxygenated hemoglobin [deoxy-Hb] and total hemoglobin [t-Hb]) calculated from the NIRS signal and changes in the Fourier Fast Transform (FFT) derived EEG alpha power as one subject goes through multiple transitions between waking and sleep. The vertical lines indicate the time of human Scored Sleep Onset and Offset. W indicates wakefulness, S indicates sleep and a.u. stands for arbitrary units.

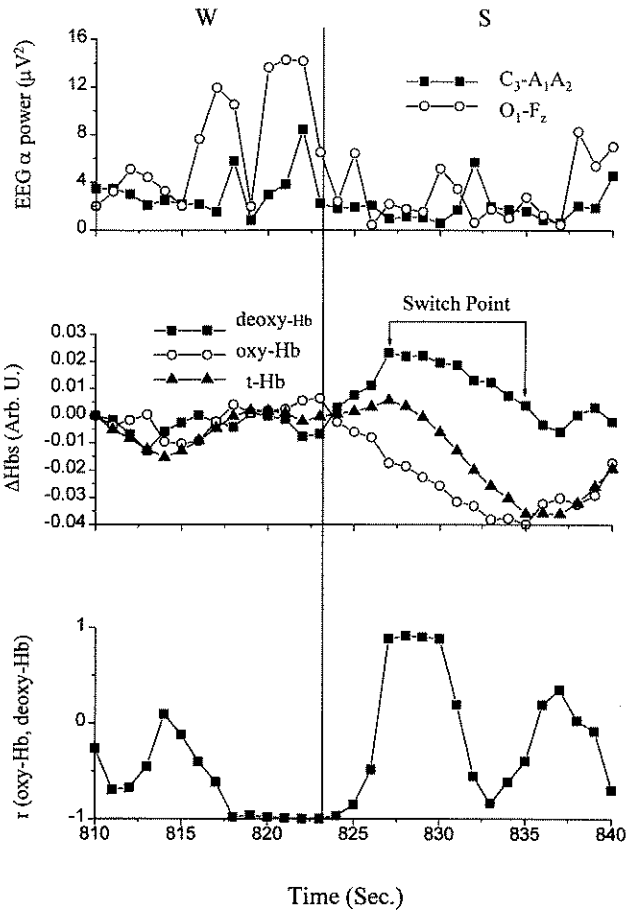

Fig. 3. Cerebral hemodynamics at sleep onset. Measurements from one subject in the transition from wakefulness to sleep. An additional curve shows the cross correlation between oxy-Hb and deoxy-Hb for a 5-s window. The axis label ΔHbs refers to the relative changes in the three hemoglobin parameters. The vertical line, at the 823rd s, indicates the point of human Scored Sleep Onset. Arrows at the 827th and 835th s point to the beginning and ending (respectively) of the synchronized reduction in both oxy-Hb and deoxy-Hb called the Switch Point. Abbreviations as in Fig. 2.

window. The value at each point represents the correlation between oxy-Hb and deoxy-Hb for the following 5-s period. As seen in the upper panel of Fig. 3, during wakefulness the alpha power of the EEG is high and as the subject falls asleep the signal becomes abruptly weaker. Four seconds after the point of Scored Sleep Onset (827 s) the levels of both oxy-Hb and deoxy-Hb begin to decrease at the same time. This fall in the two chromophores continues for 8 s (through 835 s). This synchronized fall, which we designate as the Switch Point, is clearly seen in the cross correlations with *r*s approaching 1.0 for values between 827 s and 830 s. Prior to and after the Switch Point there are small changes in oxy-Hb and deoxy-Hb. The relationship between the two chromophores in the region bordering the Switch Point is either distinctly reciprocal or mildly parallel as can be seen in the middle panel and as represented in the lower panel by *r* values approaching −1.0 and low positive values, respectively.

As expected, grouped data show highly significant reductions in EEG alpha power at both electrode locations during the transition to sleep (Table 3; Ps<0.0005). The mean point of Scored Sleep Onset was 4.7 s (S.D.$=3.9$, $t=3.29$, $n=9$, $P<0.01$) after the mean point of computer FFT Sleep Onset at the C_3–A_1A_2 placement.

The concentration of oxy-Hb was reduced in the transition to sleep (mean difference [second 5 s] minus [first 5 s]$=-0.01571$ arbitrary units, S.D.$=0.04209$, $t=3.11$, $n=9$, $P<0.01$). In contrast to this overall decrease in oxy-Hb, there were 6 of 26 nap trials in which the largest change was an increase. In order to examine the changes in deoxy-Hb and t-Hb that occurred at the time of the fall in oxy-Hb, we located the portion of the sleep onset record, in these 6 nap trials, in which there was the largest decrease in oxy-Hb. As subjects fell asleep and oxy-Hb decreased (Table 3) there was a near significant reduction in deoxy-Hb ($n=9$, $P<0.063$). Employing the nap trial as the unit of analysis, there was a significant reduction in deoxy-Hb (mean difference [second 5 s] minus [first 5 s]$=-0.00609$ arbitrary units, S.D.$=0.01315$, $t=3.47$, $n=26$, $P<0.005$). In contrast to the general reduction in deoxy-Hb at sleep onset, there were 6 of 26 nap trials in which the largest change in deoxy-Hb was an increase. At the time of the fall in oxy-Hb at sleep onset, there was also a reduction in t-Hb ($P<0.002$).

In 18 of the 26 sleep onset trials there was a Switch Point characterized by a distinct synchronized decrease in both oxy-Hb and deoxy-Hb. In the remaining 8 trials the relationship between the chromophores was either recip-

Table 3
Changes in alpha power (μV^2 units) and hemoglobin concentrations (arbitrary units) in the transition from wakefulness to sleep[a]

Parameter	Mean	S.D.	t	$P<$
ΔFFT alpha power C_3–A_1A_2 (log scale)	−1.1423	0.4145	5.56	0.0005
ΔFFT alpha power O_1–F_z (log scale)	−1.1498	0.4070	5.75	0.0005
Δoxy-Hb	−0.0386	0.0124	5.29	0.001
Δdeoxy-Hb	−0.0056	0.0126	2.00	0.063
Δt-Hb	−0.0441	0.0199	4.47	0.002

[a] The segment of the transition period where there was a maximal reduction in oxy-Hb between two successive 5-s periods was used for analysis of hemoglobin changes. The data set was based on a total of 26 observations in 9 subjects. The mean of each subject's data was used for the statistical analysis. The symbol Δ stands for change, calculated as follows: Average parameter value in the second 5-s window minus the value in the first 5 s window. Negative values mean a reduction in the parameter from wakefulness to sleep.

rocal or indeterminate. The mean duration of the Switch Point was 3.6 s (S.D. = 1.6 s, $n = 18$). The mean delay from the Scored Sleep Onset to the start of the Switch Point was 3.8 s (S.D. = 8.2, $n = 18$). The correlation between oxy-Hb and deoxy-Hb at the Switch Point was $r = 0.94$ ($n = 18$, Fig. 4). This simultaneous decrease in both chromophores results in a drop in t-Hb and probably reflects a brief down regulation of cerebral blood flow or volume at sleep onset.

Before and after the Switch Point a different NIRS pattern was seen with levels of both oxy-Hb and deoxy-Hb showing increases and decreases of small magnitude. The two chromophores showed both reciprocal changes (as one increased the other decreased) as well as parallel changes (Fig. 4). The mean correlation of the two chromophores in the 5 s before ($r = 0.04$) and the 5 s after ($r = 0.03$) the Switch Point in the region of sleep onset approached zero ($n = 18$). Therefore, the Switch Point is a distinct and fairly uniform phase of hemodynamic regulation that is bounded by a mixture of changes.

3.2. The sleep to wakefulness transition produced by forced arousal

Fig. 5 displays the data from one subject before and after being awakened. While asleep the alpha power of the EEG signals is low and abruptly increases 1 s after the point of Scored Sleep Offset at the 719th s. The synchronized increase of both oxy-Hb and deoxy-Hb (Switch Point) starts at the 723rd s and ends at the 729th s. This is also reflected in the cross correlation values approaching $r = 1.0$ between the 720th and 725th s in the lower panel. Prior to and after the Switch Point the relationship between oxy-Hb and deoxy-Hb is a mixture of reciprocal and parallel changes as reflected in the wide range of positive and negative correlations in the lower panel.

Grouped data show that as subjects wake up EEG alpha power signals increase (Table 4, $n = 9$, both Ps < 0.0005).

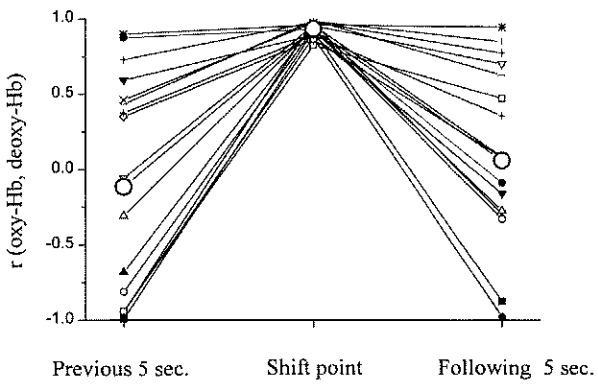

Fig. 4. Correlation of oxy-Hb and deoxy-Hb around sleep onset. The middle set of values are the standardized correlation coefficients between oxy-Hb and deoxy-Hb at each sleep onset trial during the Switch Point. The first set of standardized correlations were obtained from 5 s prior to the Switch Point and the third set from 5 s after the Switch Point. The large open circles indicate the mean values ($n = 18$).

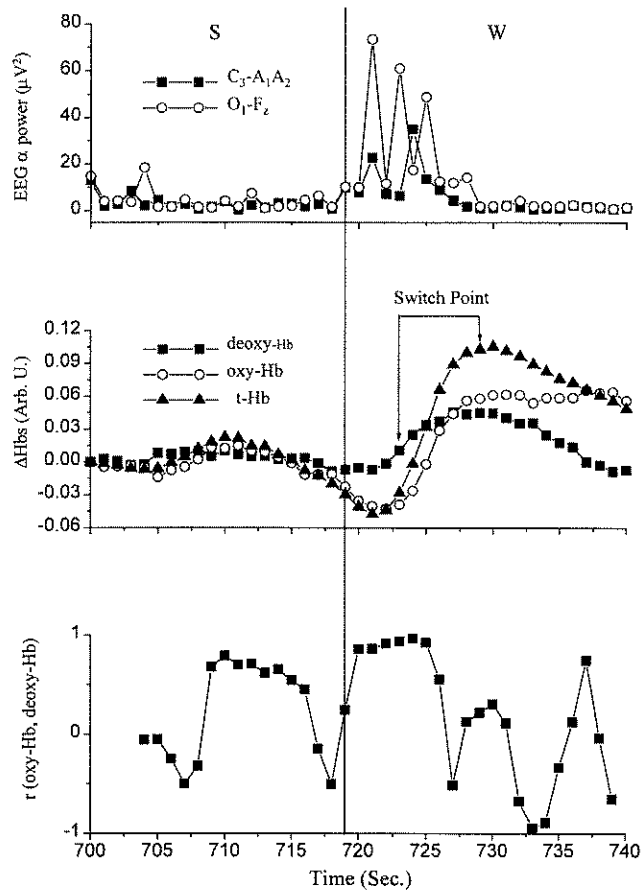

Fig. 5. Cerebral hemodynamics at sleep offset. Measurements from one subject in the transition from sleep to wakefulness. Symbols as in Fig. 3. The vertical line, at the 719th s, indicates the point of human Scored Sleep Offset. Arrows at the 723rd and 729th s point to the beginning and ending (respectively) of the synchronized increase in both oxy-Hb and deoxy-Hb called the Switch Point.

The mean point of Scored Sleep Offset occurred 4.1 s before the increase in FFT alpha power at the C_3–A_1A_2 placement (S.D. = 3.3 s, $t = 3.37$, $n = 9$, $P < 0.01$).

There was a rapid and robust increase in oxy-Hb level as subjects were awakened (mean difference [second 5 s] minus [first 5 s] = 0.08056, S.D. = 0.04680, $t = 3.94$, $n = 9$, $P < 0.005$). In contrast to the general increase in oxy-Hb,

Table 4
Changes in alpha power (μV^2 units) and hemoglobin concentrations (arbitrary units) in the transition from sleep to wakefulness[a]

Parameter	Mean	S.D.	t	$P<$
ΔFFT alpha power C_3–A_1A_2 (log scale)	1.57	0.28	7.14	0.0001
ΔFFT alpha power O_1–F_z (log scale)	1.57	0.40	5.93	0.0005
Δoxy-Hb	0.100	0.036	5.01	0.001
Δdeoxy-Hb	0.014	0.023	2.32	0.05
Δt-Hb	0.114	0.039	5.11	0.001

[a] The segment of the transition period where there was a maximal increase in oxy-Hb between two successive 5-s periods was used for analysis. The data set was based on a total of 37 observations in 9 subjects. The mean of each subject's data was used for the statistical analysis. Definitions as in Table 3.

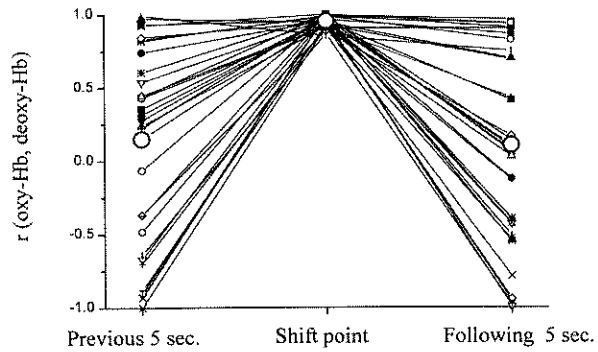

Fig. 6. Correlation of oxy-Hb and deoxy-Hb around sleep offset. Definitions as in Fig. 4. $n=32$.

there were 7 of 37 trials in which the largest change was a reduction. We located the segment of the sleep offset period in which the oxy-Hb level was increased in these 7 trials in order to analyze the accompanying NIRS changes. As subjects woke up and oxy-Hb increased (Table 4), deoxy-Hb also increased ($P<0.05$). At the time of the rise in oxy-Hb, t-Hb also increased ($P<0.001$).

In 32 of 37 trials there was a synchronized and parallel increase in both oxy-Hb and deoxy-Hb upon awakening. In the remaining 5 trials the relationship between the chromophores was reciprocal or indeterminate. The mean duration of the Switch Point was 3.4 s (S.D.=1.5, $n=32$). The correlation between oxy-Hb and deoxy-Hb at the Switch Point was $r=0.94$ ($n=32$; Fig. 6). The mean delay from the Scored Sleep Offset to the start of the Switch Point was 1.5 s (S.D.=3.8, $n=32$). There was no difference in the speed of the hemodynamic response at sleep offset and sleep onset. The time from the Scored Sleep Offset to the Switch Point (mean=1.5 s, S.D.=3.8, $n=32$) compared to the time from the Scored Sleep Onset to the Switch Point (mean=3.8 s, S.D.=8.2) was not different ($n=18$, $t=-1.28$, n.s.).

Before and after the Switch Point at sleep offset, oxy-Hb and deoxy-Hb showed small increases and decreases. The relationship between the two chromophores in the region outside the Switch Point was reciprocal as well as parallel (Fig. 6). The mean correlation between the two chromophores was small in the 5 s before ($r=0.13$) and the 5 s after ($r=0.27$) the Switch Point ($n=32$; Fig. 6).

4. Discussion

The current work has demonstrated that the global changes that occur between the states of wakefulness and sleep are accompanied by consistent changes in hemodynamics. The process of falling asleep, characterized by simultaneous reductions in the concentration of oxy-Hb and deoxy-Hb, suggests decreased neuronal activity, reduced oxygen consumption and reduced cerebral blood flow and volume [70,72]. It is not unexpected that this superficial layer of the frontal lobe, assessed by the NIR light, which is associated with emotionality and executive functioning such as planning and sequencing reduces its metabolic rate upon falling asleep. The current findings are consistent with other imaging techniques, which have shown that the type of sleep seen at the beginning of the night is associated with reduced cerebral metabolic rate as measured by PET scan [3] and reduced cerebral blood flow [16,32,46,57].

Previous studies using NIRS in frontal areas during the wakefulness to sleep transition in humans have also shown decreased oxy-Hb as in the current study [25,59]. In contrast to the current work's finding of deoxy-Hb reductions, past studies have described an increase in deoxy-Hb in the transition to sleep. This discrepancy may be due to the current work's focus on the changes in the immediate region around the transition to sleep. Our analysis was limited to the 5 s preceding and 20 s following the state changes. One past study examined longer-term changes over many minutes and therefore did not concentrate on the transient change at the boundary [25]. The other study used a sampling rate of 5 s for NIRS, which is a temporal resolution that would not be capable of detecting brief changes [59].

Alternatively, the differences between the current and past studies with regard to deoxy-Hb may be due to methodological differences. The current study examined naps during the day, in partially sleep deprived individuals as compared with nocturnal sleep in past work. In an attempt to assess this possible explanation we re-studied one of our subjects at his typical bedtime. These preliminary data show the same changes in the chromophores that we obtained during the day.

Other differences in methods between the current and past studies which include, differences in scalp locations of the optodes, the current studies selection of state transitions that were clear and uniform, and differences in the NIRS apparatus, sampling rate, and different light wavelengths employed may explain the discrepancies in findings. Only more work will settle the issue.

Although we only analyzed short segments of data we observed a pattern of small changes in oxy-Hb and deoxy-Hb both before and after the transition to sleep. The pattern was not uniform; in some trials the two chromophores were reciprocally related and in other trials parallel changes occurred. Because we did not examine longer-term trends a direct comparison to the findings of previous work is not possible.

Falling asleep is gradual as reflected in a number of parameters, including decreased tonus of the skeletal musculature and responsivity to sensory stimulation [55]. The current finding of a transient reduction of substantial magnitude in oxy-Hb coupled with a smaller reduction in deoxy-Hb that is bracketed by smaller, mixed changes suggests that cortical hemodynamics are switched abruptly into a specific mode at sleep onset.

The validity of the current findings at sleep onset is supported by the opposite results obtained when subjects are awakened from sleep. The increases in both oxy-Hb and deoxy-Hb are synchronized and time locked to the awakening period. Because we abruptly awakened subjects, the precise point of sleep offset is more distinct then sleep onset. This ease of identification may be reflected in the reduced variability in the time between Scored Sleep Offset to the Switch Point compared to Scored Sleep Onset to the Switch Point. While this difference is probably due to the sharp contrast between sleep and wakefulness at the abrupt awakening, it may also, in part, be due to the adaptive advantage of consistency of cerebral responsivity to an awakening.

Many studies employing NIRS in the evaluation of the cerebral hemodynamic response to mental activation have also shown oxy-Hb increases as we have found at sleep offset ([47], see [70]). While most studies have found that deoxy-Hb is decreased during activation [see 70] there has been one study using intrinsic optical signals and two studies using f-MRI in which activation produced an initial, short lived, increase in deoxy-Hb as we have found at sleep offset [11,34,43]. The parallel changes in both oxy-Hb and deoxy-Hb that define the Switch Point and last for approximately 3 to 4 s suggest that the vascular response takes in the order of seconds to make the switch in response to changes in neuronal demands associated with sleep and wakefulness. While the parallel and synchronized changes in oxy-Hb and deoxy-Hb at the transition between sleep and wakefulness were clearly seen they were not invariably present. In a minority of trials only small reciprocal changes occurred. It is not clear if this represents a limitation of the NIRS technique or the variability of hemodynamics at the global central nervous system change in the sleep state transition period.

Questions regarding spatial resolution, data that is limited to within subject comparisons and the possible contamination of the signal by extracerebral sources are three limitations of the current NIRS approach. A number of studies have shown that with optical imaging using the reflectance mode there is a direct relationship between optode separation and the depth of the volume of tissue interrogated [14,15,18]. The light path through the head and to the detector optode has been described as crescent or banana shaped [14,23]. For an optode separation of 3 cm used in this study, studies suggest that the depth of light penetration is 1.5–3.0 cm from the surface or less than 1 cm into brain tissue [21,23,29,41,49,71,74]. However, a recent model employing a multi-layer assumption of the tissues illuminated suggest that the light path may not be crescent shaped because of light tunneling effects through certain tissue layers [50]. Furthermore, the path of the light through the head and the volume of tissue assessed vary with individual differences, such as skin pigment and skull thickness (see [47]). Although spatial resolution has been estimated at a few cm^3, the depth and location of the anatomic site assessed remains an inference unless convergent measures are also employed [23,29,72]. This represents a problem in studies that aim to examine discrete functionally specific anatomic sites. In the current study, no claim is made that a highly circumscribed volume of cerebral tissue is responsible for the hemodynamic change in the transitions between sleep and waking.

The modified Beer–Lambert algorithm used to establish the concentration of oxy-Hb and deoxy-Hb requires the knowledge of the pathlength of the light through the tissue (see [69]). There are NIRS techniques, such as frequency domain and time-resolved methods, that assess pathlength and thus permit the derivation of absolute levels of the hemoglobin molecules [35,58]. Because the reflectance mode used in this study does not permit the determination of pathlength it is necessary to assume that this distance does not change during the measurement period. While pathlength is affected by changes in the chromophore concentrations themselves [58] this assumption of constant pathlength is reasonable in measurements taken within the individual at the same location [69]. The data thus obtained is semi-quantitative, trend data, with no absolute levels determined. Relative changes in concentration of the hemoglobin molecules within the same individual, at the same optode position are possible. Moving the optodes to a different location on the head in the same individual or to a different subject will necessarily void the assumption of constant light pathlength and obviate comparisons of absolute amplitudes of the chromophores. This limits the applicability of this reflectance mode method. The within subject design of the current work avoids the problem of individual differences.

It is clear that extracranial sources of light absorption such as blood in skin, bone and fascia contribute to the NIRS signal [13,17,28] although controversy exists regarding the extent of this contribution. Psychomotor studies that show contralateral and no unilateral changes in NIRS as well as the convergent validity studies of NIRS with PET and fMRI are among the numerous studies that provide evidence for the intracerebral source of the signal [21,23,29,72]. With interoptode separation of 3 cm or more the extracerebral contribution to NIRS parameters is small according to some studies [49,61,73]. While the current study's interoptode separation and probe pressure reducing blood flow in the skin may limit non-cerebral sources from the NIRS signal, the extracerebral sources were not assessed. Therefore, the current result may not be interpreted as due solely to hemodynamic changes at the frontal pole of the cortex.

In summary, a synchronized, parallel change in oxy-Hb and deoxy-Hb is a discrete event that occurs in the transition from both sleep to wakefulness and wakefulness to sleep. The major source of these changes measured in this study is the cerebral cortex at the frontal pole. This transient and abrupt change in cerebral hemodynamics

resembles a switch process that resets the concentration of both chromophores to a new level; lower at sleep onset and higher at sleep offset. To the extent that these changes in the optical density of these hemoglobin molecules represent changes in cerebral blood flow or volume they reflect the different perfusion demands of these different states.

Acknowledgements

This study was partially supported by the Department of Energy, Medical Laser Center of Excellence Program and Mediscience Technology Corp.

References

[1] A.R. Braun, T.J. Balkin, N.J. Wesenten, R.E. Carson, M. Varga, P. Baldwin, S. Selbie, G. Belenky, P. Herscovitch, Regional cerebral blood flow throughout the sleep–wake cycle: An $H_2^{15}O$ PET study, Brain 120 (1997) 1173–1197.

[2] J.E. Brazy, D.V. Lewis, M.H. Mitnick, F.F. Jobsis, Non-invasive monitoring of cerebral oxygenation in preterm infants: preliminary observations, Pediatrics 75 (1985) 217–225.

[3] M.S. Buchsbaum, J.C. Gillin, J. Wu, E. Hazlett, N. Sicotte, R.M. Dupont, W.E. Bunney Jr., Regional cerebral glucose metabolic rate in human sleep assessed by positron emission tomography, Life Sci. 45 (1989) 1349–1356.

[4] M.S. Buchsbaum, W.B. Mendelson, W.C. Duncan, R. Coppola, J. Kelsoe, J.C. Gillin, Topographic cortical mapping of EEG sleep stages during daytime naps in normal subjects, Sleep 5 (3) (1982) 248–255.

[5] B. Chance, J.S. Leigh, H. Miyake, D. Smith, S. Nioka, R. Greenfeld, M. Finander, K. Kaufmann, W. Levy, M. Young, Comparison of time resolved and un-resolved measurements of deoxyhemoglobin in brain, Proc. Natl. Acad. Sci. 85 (1988) 4971–4975.

[6] B. Chance, Optical method, Annu. Rev. Biophys. Chem. 20 (1991) 1–28.

[7] J. Cohen, C. Cohen, Applied Multiple Regression/Correlation Analysis for the Behavioral Sciences, Lawrence Erlbaum, NY, 1975, 490.

[8] T. Delpy, M.C. Cope, E.B. Cady, J.S. Wyatt, P.A. Hamilton, P.L. Hope, S. Wray, E.O.R. Reynolds, Cerebral monitoring in newborn infants by magnetic resonance and near infrared spectroscopy, Scand. J. Clin. Lab. Invest. 47 (Suppl 188) (1987) 9–17.

[9] D.T. Delpy, M. Cope, P. van der Zee, S. Arridge, S. Wray, J. Wyatt, Estimation of optical path length, Phys. Med. Biol. 33 (1988) 1433–1442.

[10] D.W. Droste, W. Berger, E. Schuler, J.K. Krauss, Middle cerebral artery blood flow velocity in healthy persons during wakefulness and sleep: A transcranial doppler study, Sleep 16 (7) (1993) 603–609.

[11] T. Ernst, J. Henning, Observation of a fast response in functional MR, Magn. Reson. Med. 32 (1994) 146–149.

[12] M. Ferrari, D.A. Wilson, D.F. Hanley, J.F. Hartmann, M.C. Rogers, R.J. Traystman, Noninvasive determination of hemoglobin saturation in dogs by derivative near-infrared spectroscopy, Am. J. Physiol. 256 (5 part 2) (1989) H1493–H1499.

[13] T.J. Germon, P.D. Evans, A.R. Manara, N.J. Barnett, P. Wall, R.J. Nelson, Sensitivity of near infrared spectroscopy to cerebral and extra-cerebral oxygenation changes is determined by emitter–detector separation, J. Clin. Monitoring Computing 14 (1998) 353–360.

[14] G. Gratton, J.S. Maier, M. Fabiani, W.M. Mantulin, E. Gratton, Feasibility of intracranial near-infrared optical scanning, Psychophysiology 31 (1994) 211–215.

[15] G. Gratton, M. Fabiani, P.M. Corballis, Can we measure correlates of neuronal activity with non-invasive optical methods? in: A. Villringer, U. Dirnagl (Eds.), Optical Imagining of Brain Function and Metabolism II, Plenum Press, New York, 1997, pp. 53–62.

[16] G. Hajak, J. Klingelhöfer, M. Schulz-Varszegi, G. Matzander, D. Sander, B. Conrad, E. Rüther, Relationship between cerebral blood flow velocities and cerebral electrical activity in sleep, Sleep 17 (1) (1994) 11–19.

[17] D.N.F. Harris, F.M. Cowans, D.A. Wertheim, NIRS in the temporal region — strong influence of external carotid artery, in: P. Vaupel et al. (Ed.), Oxygen Transport to Tissue XV, Plenum Press, New York, 1994, pp. 825–828.

[18] D.N.F. Harris, F.M. Cowans, D.A. Wertheim, S. Hamid, NIRS in adults — Effects of increasing optode separation, in: P. Vaupel et al. (Ed.), Oxygen Transport to Tissue XV, Plenum Press, New York, 1994, pp. 837–840.

[19] T. Hayakawa, M. Terashima, Y. Kayukawa, T. Ohta, T. Okada, Changes in cerebral oxygenation and hemodynamics during obstructive sleep apneas, Chest 109 (4) (1996) 916–921.

[20] J. Hazan, R. Broughton, Quantitative topographic EEG mapping during drowsiness and sleep onset, in: R.D. Ogilvie, J.R. Harsh (Eds.), Sleep Onset: Normal and Abnormal Processes, American Psychological Association, Washington DC, 1994, pp. 219–235.

[21] C. Hirth, H. Obrig, K. Villringer, A. Thiel, J. Bernarding, W. Muhlnickel, H. Flor, U. Dirnagl, A. Villringer, Non-invasive functional mapping of the human cortex using near-infrared spectroscopy, NeuroReport 7 (1996) 1977–1981.

[22] W.D. Heiss, G. Pawlik, K. Herholz, R. Wagner, K. Wienhard, Regional cerebral glucose metabolism in man during wakefulness, sleep, and dreaming, Brain Res. 327 (1985) 362–366.

[23] C. Hock, K. Villringer, F. Müller-Spahn, R. Wenzel, H. Heekeren, S. Schuh-Hofer, M. Hofmann, S. Minoshima, M. Schwaiger, U. Dirnagl, A. Villringer, Decrease in parietal cerebral hemoglobin oxygenation during performance of a verbal fluency task in patients with Alzheimer's disease monitored by means of near-infrared spectroscopy (NIRS) — correlation with simultaneous rCBF—PET measurements, Brain Res. 755 (1997) 293–303.

[24] C.C. Hong, J.C. Gillin, B.M. Dow, J. Wu, M.S. Buchsbaum, Localized and lateralized cerebral glucose metabolism associated with eye movement during REM sleep and wakefulness: A positron emission tomography (PET) study, Sleep 18 (7) (1995) 570–580.

[25] Y. Hoshi, S. Mizukami, M. Tamura, Dynamic features of hemodynamic and metabolic changes in the human brain during all-night sleep as revealed by near-infrared spectroscopy, Brain Res. 652 (1994) 257–262.

[26] H. Jasper, Report of the committee on methods of clinical examination in electroencephalography, Electroencephalogr. Clin. Neurophysiol. 10 (1959) 370–375.

[27] F.F. Jobsis, Noninvasive, infrared monitoring of cerebral and myocardial oxygen sufficiency and circulatory parameters, Science 198 (4323) (1977) 1264–1267.

[28] P.J. Kirkpatrick, P. Smielewski, J.M.K. Lam, P. Al-Rawi, Use of near infrared spectroscopy for the clinical monitoring of adult brain, J. Biomedical. Optics 1 (4) (1996) 363–372.

[29] A. Kleinschmidt, H. Obrig, M. Requardt, K.D. Merboldt, U. Dirnagl, A. Villringer, J. Frahm, Simultaneous recording of cerebral blood oxygenation changes during human brain activation by magnetic resonance imaging and near-infrared spectroscopy, J. Cerebr. Blood Flow Metab. 16 (5) (1996) 817–826.

[30] C.D. Kurth, J.M. Steven, D. Benaron, B. Chance, Near-infrared monitoring of the cerebral circulation, J. Clin. Monit. 9 (1993) 163–170.

[31] Laser Institute of America, American National Standards for Use of Lasers, ANSI., Table 6, p. 42, Table 7, p. 43, Z136.1, 1993.

[32] P.L. Madsen, J.F. Schmidt, S. Holm, S. Vorstrup, N.A. Lassen, G.

Wildschiodtz, Cerebral oxygen metabolism and cerebral blood flow in man during light sleep (stage 2), Brain Res. 557 (1991) 217–220.
[33] P.L. Madsen, J.F. Schmidt, G. Wildschiodtz, L. Friberg, S. Holm, S. Vorstrup, N.A. Lassen, Cerebral oxygen O_2 metabolism and cerebral blood flow in humans during deep and rapid-eye-movement sleep, J. Appl. Physiol. 70 (6) (1991) 2597–2601.
[34] D. Malonek, A. Grinvald, Interactions between electrical activity and cortical microcirculation revealed by imaging spectroscopy: Implications for functional brain mapping, Science 272 (1996) 551–554.
[35] W.W. Mantulin, J.B. Fishkin, P.T.C. So, E. Gratton, J.S. Maier, Quantitative diffusive wave spectroscopy in tissues, SPIE Proceedings 1888 (1993) 420–427.
[36] P. Maquet, Positron emission tomography studies of sleep and sleep disorders, J. Neurol. 244 (Suppl. 1) (1997) S23–S28.
[37] P. Maquet, D. Dive, E. Salmon, B. Sadzot, G. Franco, R. Poirrier, R. von Frenckell, G. Franck, Cerebral glucose utilization during sleep–wake cycle in man determined by positron emission. tomography and [18F]2-fluoro-2-deoxy-D-glucose method, Brain Res. 513 (1990) 136–143.
[38] P. Maquet, C. Phillips, Functional brain imaging of human sleep, J. Sleep Res. 7 (Suppl. 1) (1998) 42–47.
[39] P.W. McCormick, M. Stewart, M.G. Goetting, G. Balakrishnan, Regional cerebrovascular oxygen saturation measured by optical spectroscopy in humans, Stroke 22 (1991) 596–602.
[40] P.W. McCormick, M. Stewart, M.G. Goetting, M. Dujovny, G. Lewis, J.I. Ausman, Noninvasive cerebral optical spectroscopy for monitoring cerebral oxygen delivery and hemodynamics, Critical Care Med. 19 (1) (1991) 89–97.
[41] P.W. McCormick, M. Stewart, G. Lewis, M. Dujovny, J.I. Ausman, Intracerebral penetration of infrared light, J. Neuorsurg. 76 (1992) 315–318.
[42] P.W. McCormick, M. Stewart, P. Ray, G. Lewis, M. Dujovny, J.I. Ausman, Measurement of regional cerebrovascular haemoglobin oxygen saturation in cats using optical spectroscopy, Neurol. Res. 13 (1) (1991) 65–70.
[43] R.S. Menon, S. Ogawa, X. Hu, J.P. Strupp, P. Anderson, K. Ugurbil, BOLD based functional MRI at 4 tesla includes a capillary bed contribution: Echo-planar imaging correlates with previous optical imaging using intrinsic signals, Magn. Reson. Med. 33 (3) (1995) 453–459.
[44] H. Merica, J.M. Gaillard, The EEG of the sleep onset period in insomnia: A discriminant analysis, Physiology & Behavior 52 (1992) 199–204.
[45] J.S. Meyer, F. Sakai, I. Karacan, S. Derman, M. Yamamoto, Sleep apnea narcolepsy, and dreaming: Regional cerebral hemodynamics, Ann. Neurol. 7 (1980) 479–485.
[46] J.S. Meyer, Y. Ishikawa, T. Hata, I. Karacan, Cerebral blood flow in normal and abnormal sleep and dreaming, Brain and Cognition 6 (1987) 266–294.
[47] H. Obrig, A. Villringer, Near-infrared spectroscopy in functional activation studies. Can NIRS demonstrate cortical activation, in: A. Villringer, U. Dirnagl (Eds.), Optical Imaging of Brain Function and Metabolism II, Plenum Press, New York, 1997, pp. 113–127.
[48] M. Ohnishi, N. Kusakawa, S. Masaki, K. Honda, N. Hayashi, Y. Shimada, I. Fujimoto, K. Hirao, Measurement of hemodynamics of auditory cortex using magneto-encephalography and near infrared spectroscopy, Acta Otolaryngol (Stockh). 532 (Suppl) (1997) 129–131.
[49] E. Okada, M. Firbank, D.T. Delpy, The effect of overlying tissue on the spatial sensitivity profile of near infrared spectroscopy. Phys. Med. Biol. 40 (1995).
[50] E. Okada, M. Firbank, M. Schweiger, S.R. Arridge, M. Cope, D.T. Delpy, A theoretical and experimental investigation of near infrared propagation in a model of the adult head, Appl. Optics. 36 (1997) 21–31.
[51] R.D. Ogilvie, J.R. Harsh (Eds.), Sleep Onset: Normal and Abnormal Processes, American Psychological Association, Washington DC, 1994, 397 pp.
[52] R.D. Ogilvie, I.A. Simons, R.H. Kuderain, T. MacDonald, J. Rustenburg, Behavioral, event-related potential, and EEG/FFT changes at sleep onset, Psychophysiology 28 (1) (1991) 54–64.
[53] S. Punwani, R.J. Ordidge, C.E. Cooper, P. Amess, M. Clemence, MRI measurements of cerebral deoxyhaemoglobin concentration [dHb]-correlation with near infrared spectroscopy (NIRS), NMR Biomed. 11 (6) (1998) 281–289.
[54] M.E. Raichle, Visualizing the mind, Scientific American, April (1994) 58–64.
[55] A. Rechtschaffen, Sleep onset: Conceptual Issues, in: R.D. Ogilvie, J.R. Harsh (Eds.), Sleep Onset: Normal and Abnormal Processes, American Psychological Association, Washington DC, 1994, pp. 3–17.
[56] A. Rechtschaffen, A.A. Kales (Eds.), Manual of standardized terminology, techniques, and scoring system for sleep stages of human subjects, National Institute of Health, Bethesda (MD), 1968, 57 pp.
[57] F. Sakai, J.S. Meyer, I. Karacan, S. Derman, M. Yamamoto, Normal human sleep: Regional cerebral Hemodyamics, Ann. Neurol. 7 (1980) 471–478.
[58] E.M. Sevick, B. Chance, J. Leigh, S. Nioka, M. Maris, Quantitation of time- and frequency-resolved optical spectra for the determination of tissue oxygenation, Anal. Biochem. 195 (1991) 330–351.
[59] S. Shiotsuka, Y. Atsumi, S. Ogata, R. Yamamoto, M. Igawa, K. Takahashi, H. Hirasawa, K. Koyama, A. Maki, Y. Yamashita, H. Koizumi, M. Toru, Cerebral blood volume in the sleep measured by near-infrared spectroscopy, Psychiatry Clin. Neurosci. 52 (2) (1998) 172–173.
[60] L. Skov, O. Pryds, G. Greisen, Estimating cerebral blood flow in newborn infants: Comparison of near infrared spectroscopy and 133Xe clearance, Pediatr. Res. 30 (6) (1991) 570–573.
[61] L. Skov, J. Ryding, O. Pryds, G. Greisen, Changes in cerebral oxygenation and cerebral blood volume during endotracheal suctioning in ventilated neonates, Acta Paediatr. 81 (1992) 389–393.
[62] P. Smielewski, P. Kirkpatrick, P. Minhas, J.D. Pickard, M. Czosnyka, Can cerebrovasular reactivity be measured with near-infrared spectroscopy?, Stroke 26 (12) (1995) 2285–2292.
[63] D.S. Smith, W. Levy, M. Maris, B. Chance, Reperfusion hyperoxia in brain after circulatory arrest in humans, Anesthesiology 73 (1990) 12–19.
[64] M.R. Stankovic, G. Zhang, A. Katz, W. Rosenfeld, P.G. Stubblefield, D. Maulik, R.R. Alfano, Continuous wave and frequency domain brain perfusion measurements: A cross-correlation animal study, Optical Society of America, Annual Meeting, Sept. 29, (1999), Santa Clara, CA.
[65] M. Tamura, O. Hazeki, S. Nioka, B. Chance, D.S. Smith, The simultaneous measurements of tissue oxygen concentration and energy state by near-infrared and nuclear magnetic resonance spectroscopy, Exp. Med. Biol 222 (1988) 359–363.
[66] A.W. Toga, J.C. Mazziotta (Eds.), Brain Mapping: The Methods, Academic Press, San Diego, 1996, 471 pp.
[67] R.E. Townsend, P.N. Prinz, W.D. Obrist, Human cerebral blood flow during sleep and waking, J. Appl. Physiol. 35 (5) (1973) 620–625.
[68] O.W. van Assendelft, Spectrophotometry of haemoglobin derivatives, Cherls C. Thomas, Assen, The Netherlands, pp. 55–57, 1970, 151 pp.
[69] P. Van der Zee, M. Cope, S.R. Arridge, M. Essenpreis, L.A. Potter, A.D. Edwards, J.S. Wyatt, D.C. McCormick, S.C. Roth, E.O.R. Reynolds, D.T. Delpy, Experimentally measured optical pathlengths for the adult head, calf and forearm and the head of the newborn infant as a function of inter optode spacing, in: T.K. Goldstick, M.M.L. Cabe, D.J. Maguire (Eds.), Oxygen Transport to Tissue XIII, Plenum Press, New York, 1992, pp. 143–153.
[70] A. Villringer, Functional neuroimaging: Optical approaches, in: A. Villringer, U. Dirnagl (Eds.), Optical Imaging of Brain Function and Metabolism II, Plenum Press, New York, 1997, pp. 1–18.

[71] A. Villringer, B. Chance, Non-invasive optical spectroscopy and imagining of human brain function, Trends Neurosci. 20 (10) (1997) 435–442.

[72] A. Villringer, U. Dirnagl, Coupling of brain activity and cerebral blood flow: Basis of functional neuroimaging, Cereb. Brain Metab. Rev. 7 (1995) 240–276.

[73] A. Villringer, J. Planck, C. Hock, L. Schleinkofer, U. Dirnagl, Near infrared spectroscopy (NIRS): a new tool to study hemodynamic changes during activation of brain function in human adults, Neurosci. Lett. 154 (1993) 101–104.

[74] K. Villringer, S. Minoshima, C. Hock, H. Obrig, S. Ziegler, U. Dirnagl, M. Schwaiger, A. Villringer, Assessment of local brain activation, in: U. Villringer A Dirnagl (Ed.), Optical Imaging of Brain Function and Metabolism II, Plenum Press, New York, 1997, pp. 149–153.

[75] K.P. Wright Jr., P. Badia, A. Wauquier, Topographical and temporal patterns of brain activity during the transition from wakefulness to sleep, Sleep 18 (10) (1995) 880–889.

[76] C.W. Yoxall, A.M. Weindling, N.H. Dawani, I. Peart, Measurement of cerebral venous oxyhemoglobin saturation in children by near-infrared spectroscopy and partial jugular venous occlusion, Pediatr. Res. 38 (1995) 319–323.

[77] G. Zhang, A.J. Spielman, P. D'Ambrosio, J. Birnbaum, S. Serizawa, D. Conroy, G. Lombardo, R.R. Alfano, The cerebral hemodynamics of obstructive sleep apnea probed by Near-Infrared Spectroscopy (NIRS), Sleep 22 (Suppl) (1998) S257.